Nonlinear Analysis and Computer Simulations
https://www.sciltp.com/journals/nacs

Article

A Robust Computational Algorithm for a Class of Nonlinear Enzyme Flow Calorimetric Models Using Taylor Wavelets: An Operational Matrix Method

K. Harvinth, S. Kavipriya, R. Seethalakshmi and G. Hariharan *

Department of Mathematics, School of Arts, Sciences, Humanities & Education (SASHE), SASTRA Deemed University, Thanjavur 613401, Tamilnadu, India
* Correspondence: hariharan@maths.sastra.edu

How To Cite: Harvinth, K.; Kavipriya, S.; Seethalakshmi, R.; et al. A Robust Computational Algorithm for a Class of Nonlinear Enzyme Flow Calorimetric Models Using Taylor Wavelets: An Operational Matrix Method. *Nonlinear Analysis and Computer Simulations* **2026**, *1*(3), 14. https://doi.org/10.53941/nacs.2026.100014

Received: 11 April 2026
Revised: 1 June 2026
Accepted: 22 June 2026
Published: 17 August 2026

Abstract: This paper discusses a mathematical model of the hysteresis behavior of the enzyme-substrate system in enzyme flow calorimetry. The hysteresis of the enzyme-substrate system due to enzyme flow calorimetry is based on the mathematical modeling of an immobilized enzyme system. The models are represented by the nonlinear differential equations of substrate inhibition kinetics in the enzymatic reaction. Two reliable wavelet-based computational algorithms for the approximate solutions for substrate concentration in planar, cylindrical, and spherical particles under steady-state conditions are discussed. To the best of our knowledge, no rigorous wavelet-based solution has been reported for the above models. The main idea of the proposed Taylor Wavelet Method (TWM) is that the nonlinear differential equations are converted into a system of algebraic equations. The validity and applicability of the proposed method are confirmed by comparing the results with those obtained by the Homotopy Perturbation Method (HPM) and the fourth-order Runge-Kutta (RK) method. Satisfactory agreement with the available results is observed. Moreover, the Chebyshev and Taylor wavelet methods are found to be efficient, simple, and straightforward tools for solving nonlinear reaction-diffusion models arising in bioprocess engineering.

Keywords: immobilized enzyme; planar particle; cylindrical particle; spherical particle; wavelets; substrate concentration

2020 MSC: 65T60; 75R50; 35K57; 33C45

1. Introduction

In modern biotechnology, physical and/or chemical enzyme immobilization in permeable solid supports is an interesting challenge. Through numerous reaction cycles, it enables the revival and reuse of the enzyme, thus minimizing global production expenses and providing an eco-friendly technology. Moreover, operation at high temperatures and in the presence of organic or ionic solvents and extreme pH conditions is enabled by enzyme stabilization [1]. Enzymes work best if there is a plethora of substrates. The rate of enzyme activity increases as the concentration of the substrate increases. However, a continuous increase in substrate concentration does not affect the activity as there are not enough enzyme molecules available to break down the excess substrate molecules. Some considerations must be taken into account after enzyme immobilization. Conformational changes caused by the interaction between the enzyme and the support matrix may cause a difference in the reaction kinetics of soluble and immobilized enzymes [2,3].

Manjón et al. [4] established the effectiveness factor for immobilized enzyme fixed-bed reactors. Vos et al. [5] discussed the effectiveness factor for spherical biofilm catalysts. Bódalo et al. [6] analyzed the diffusion effects of immobilized enzymes on porous supports with reversible Michaelis-Menten kinetics. Gómez et al. [7] developed a two-parameter model for evaluating the effectiveness factor for immobilized enzymes with reversible Michaelis–Menten kinetics. An analytical expression of the effectiveness factor for immobilized enzyme systems with reversible Michaelis-Menten kinetics established by Rani et al. [8]. The homotopy perturbation method (HPM) is a promising new-age semi-analytical method to obtain solutions to nonlinear ODEs. The method consists of expanding the relevant variables and some parameters if needed, as well as power series depending on the homotopy parameter (p). The method has proved to be vastly effective, but they are yet to study related to the comparison of experimental data or its application in multi-substrate reactions. The Runge-Kutta (RK) method is a conventional numerical method used for obtaining approximate solutions to reaction-diffusion equations. However, it requires a high computational cost, which increases with decreasing Thiele modulus, especially when the boundary conditions involve mass transfer due to convection forces.

Wavelet theory is an emerging area in applied mathematical research. Avudainayagam and Vani [9] applied the wavelet-Galerkin method for solving integro-differential equations. Wavelets have been applied in engineering disciplines, such as signal analysis for waveform representation and segmentation, harmonic analysis, time-frequency analysis, etc. In computational algorithms, wavelet-based methods and hybrid methods become important tools because of the properties of localization. Goyal and Mehra [10] applied an adaptive meshfree spectral graph wavelet method for partial differential equations. Guf and Jiang [11] established the Haar wavelet method for solving differential equations. Razzaghi and Yousefi [12] introduced the Legendre wavelet operational matrix of integration. Keshavarz and Ordokhani [13,14] used the Taylor wavelet method for solving integro-differential equations and boundary value problems. Toan [15] applied the Wavelet method for fractional delay differential equations. Pandy Prabaharan [16] applied the wavelet method for estimating the concentration of species and effectiveness. Sivasankari and Rajendran [17] established the analytical expressions of the concentration of species and effectiveness factors in porous catalysts using the Adomian decomposition method. For the past 15 years, Hariharan and his co-workers [16,18–22] have established discrete wavelet-based computational algorithms for solving nonlinear and fractional differential equation models. Yousefi [23] used the Legendre wavelets methods for solving differential equations of Lane-Emden type. Yin Yang [24] solved a nonlinear multi-order fractional differential equation using Legendre Pseudo-spectral methods. Mohammadi [25] established an extended Legendre Wavelet method for solving differential equation. Excellent summaries are provided for wavelet transform method and their applications in science and engineering (See Refs. [26,27]). Chitra Devi et al. [28] applied the Homotopy perturbation method to find the analytical expressions for substrate concentrations with various parameter values.

In this paper, an efficient analytic solution of the proposed model is obtained by using the Taylor wavelet method, which has been applied to find approximate solutions of nonlinear reaction-diffusion equations. It is also worth mentioning that the proposed wavelet method is computationally more effective since the defining domain is finite and the operational matrix is tridiagonal. The weight function is orthogonal, and the convergence is rapid.

The paper is organized as follows. In Section 2, the Mathematical formulation of the given problem is given. In Section 3, Taylor wavelets and their properties are discussed. The method of solution by the Taylor wavelet is presented in Section 4. Results and discussions are presented in Section 5. Concluding remarks and future scope are given in Section 6.

2. Mathematical Formulation of the Problem

The nonlinear differential equation for a spherical particle within the enzymatic layer for the steady state concentration is described by

$$\frac{d^2S_c}{dr^2}+\frac{2}{r}\frac{dS_c}{dr}-\frac{V_mS_c}{D_e\left(K_m+S_c+\frac{S_c{}^2}{k_i}\right)}=0, \tag{1}$$

where S_c is the substrate concentration, r is the particle radial coordinate, V_m is the Michaelis constant and k_i is the substrate inhibition constant.

The boundary conditions associated with this model are

$$\frac{dS_c}{dr}=0 \text{ at } r=0 \tag{2}$$

$$S_c=S_{c0} \text{ at } r=R_p \tag{3}$$

where R_p denotes the particle diameter and S_{c0} is the substrate concentration at the particle surface.

Consider the dimensionless quantities,

$$S = \frac{S_c}{K_m},\ x = \frac{r}{R_p},\ \phi = R_p\sqrt{\frac{V_m}{K_m D_e}},\ \beta = \frac{k_i}{K_m}, C_0 = \frac{S_{c0}}{K_{m.}}$$

Substituting these variables into Equation (1) leads to the dimensionless concentration of substrate for a spherical particle

$$\frac{d^2 S_c}{dx^2} + \frac{2}{x}\frac{dS_c}{dx} - \phi^2 \frac{S}{1+S+\frac{S^2}{\beta}} = 0 \tag{4}$$

where S is the dimensionless substrate concentration, x is the dimensionless particle radial coordinate, ϕ is the Thiele modulus and β is the dimensionless kinetic parameter. The corresponding dimensionless boundary conditions are

$$\frac{dS}{dx} \text{ at } x = 0. \tag{5}$$

$$S = S_0 \text{ at } x = 1$$

where S_0 is the dimensionless substrate concentration at the particle surface. For the case of the planar and cylindrical particles, the dimensionless forms of Equation (1) are respectively, given by

$$\frac{d^2 S}{dx^2} - \phi^2 \frac{S}{1+S+\frac{S^2}{\beta}} = 0 \tag{6}$$

$$\frac{d^2 S}{dx^2} + \frac{2}{x}\frac{dS}{dx} - \phi^2 \frac{S}{1+S+\frac{S^2}{\beta}} = 0 \tag{7}$$

with the same boundary conditions for the planar and cylindrical particles as given in equations. The effect of mass transfer on the reaction rate is determined by the effectiveness factor η given by $\eta = \frac{V_p}{V(S_{c0})}$, where V_p denotes the overall particle reaction rate and $V(S_{c0})$ represents the rate, which would be obtained with no diffusion limitation in the biocatalyst particle, that is

$$V(S_{c0}) = \frac{V_m S_{c0}}{K_m + S_{c0} + \frac{{S_{c0}}^2}{k_i}} \tag{8}$$

After dimensioning, the effectiveness factor takes the form

$$\eta = \frac{3(dS/dx)_{x=1}}{\phi^2 S_0/(1+S_0+\frac{S^2{}_0}{\beta})}$$

3. Taylor Wavelets and Properties

Wavelets constitute a family of functions constructed from dilation and translation of a single function called the mother wavelet. When the dilation parameter and the translation parameter are continuously, we have the following family of continuous wavelets $\psi_{a,b}(t) = |a|^{-\frac{1}{2}}\psi\left(\frac{x-b}{a}\right)$, $a, b \in R$.

Taylor wavelets $\psi_{nm}(t) = \psi(k, \hat{n}, m, t)$ have four arguments; $\hat{n} = n - 1, n = 1,2,3,\dots, 2^{k-1}$, k can assume any positive integer, m is the order for Taylor polynomials and t is the normalized time. They are defined on the interval $[0, 1)$ by:

$$\psi_{nm}(t) = \begin{cases} 2^{\frac{k-1}{2}} T_m(2^{k-1}t - \hat{n}), \frac{\hat{n}}{2^{k-1}} \leq t < \frac{\hat{n}+1}{2^{k-1}}, \\ 0, otherwise \end{cases}$$

where $\tilde{T}_m(t) = \sqrt{2m+1}T_m(t)$, where m = 0, 1, 2, …, $M - 1$ and $n = 1, 2, 3, \dots,\ 2^{k-1}$. The coefficient $\sqrt{2m+1}$ is for normality. Here, $T_m(t)$ are the well-known Taylor polynomials of order m which can be defined by $T_m(t) = t^m$. Taylor polynomials form a complete basis over the interval [0,1].

3.1. Function Approximation

A function $f(t)$ defined over [0,1] may be expanded in terms of Taylor wavelets as

$$f(t) = \sum_{n=1}^{\infty} \sum_{m=0}^{\infty} C_{nm}\psi_{nm}(t) \tag{9}$$

where $c_{nm} = (f(x), \psi_{nm}(t))$ in which (.,.) denotes the inner product. If the infinite series in (9) is truncated, then it can be written as

$$f(t) = \sum_{n=0}^{2^{k-1}} \sum_{m=0}^{M-1} C_{nm}\psi_{nm}(t) = C^T\psi(t) \tag{10}$$

where C and $\psi(t)$ are $2^k(M + 1) \times 1$ defined by

$$C = [c_{0,0}, c_{0,1}, \dots, c_{0,M}, \dots, c_{2^k-1,M}, \dots, c_{2^k-1,1}, \dots, c_{2^k-1,M}]^T$$

$$\psi(t) = [\psi_{0,0}, \psi_{0,1}, \dots, \psi_{0,M}, \dots \psi_{2^k-1,M}, \dots, \psi_{2^k-1,1}, \dots, \psi_{2^k-1,M}]^T$$

3.2. Error Analysis

Here, we obtain the error bound of the approximate $f(x)$ by using Taylor wavelet series.

Theorem 1. *Let $f(x) \in C^p[a,b]$ and $S_p(x)$ be the interpolating polynomial of degree p which agrees with f(x) at the Chebyshev nodes on [a,b], then*

$$|f(x) - S_p(x)| \leq \frac{2}{p!}\left(\frac{b-a}{4}\right) max_{\tau\epsilon[a,b]}\left|f^{(p)}(\tau)\right| \tag{11}$$

Theorem 2. *Let $f(x) \in C^p[a,b]$ and $f(x) \approx \sum_{n=1}^{2^{k-1}} \sum_{m=0}^{M-1} c_{nm\psi_{nm}}(x) = C^T\psi(x)$. Then the error bound would be obtained as follows*

$$\|f(x) - C^T\psi(x)\| \leq \frac{2}{p!4^p2^{p(k-1)}} max\,|f^p(\tau)|.$$

Theorem 3. *Let Ψ (t) be the Taylor wavelets vector defined, Then the first derivative of the vector Ψ (t) can be expressed as*

$$\frac{d\psi(t)}{dt} = D\psi(t)$$

where D is $2^k(M + 1)$ square matrix of derivatives and is defined by

$$D = \begin{bmatrix} F & O & . & . & . & O \\ O & F & . & . & . & O \\ . & . & . & . & . & . \\ . & . & . & . & . & . \\ O & O & . & . & . & F \end{bmatrix}$$

in which F is an (M + 1) square matrix and its (r,s)th element is defined by

$$F_{r,s} = \begin{cases} 2^{k+2}s, & r \geq 2, r > s \text{ and } (r+s) \text{ odd} \\ 0 & otherwise \end{cases}$$

Corollary 1. *The operational matrix for the nth derivative can be obtained from*

$$\frac{d^n\psi(t)}{dt^n} = D^n\psi(t),\ n = 1,2, \dots..$$

where D^n is the n^{th} power of D.

4. Method of Solution by the Taylor Wavelet Method (TWM)

We consider the IVP

$$y''(x) + \frac{a}{x}y'(x) + f\big(x, y(x)\big) = 0 \tag{12}$$

Subject to the initial conditions

$$y(0) = k_1, y'(0) = k_2, \tag{13}$$

where α, k_1 and k_2 are real numbers, and $f(x, y(x))$ is a given continuous real valued function.

In order to solve the indicated type of equation, the solution of Equation is expressed as follows

$$y(x) = \sum_{n=1}^{2^{k-1}} \sum_{m=0}^{M-1} c_{nm}\varphi_{nm}(x) = D\phi(x) \tag{14}$$

Hence,

$$y'(x) = D\phi'(x) \text{ and } y''(x) = D\phi''(x)$$

where $D, \phi(x), \phi'(x), \phi''(x)$ are in the form

$$D = \left[c_{10}, c_{11}, \dots, c_{1(M-1)}, c_{20}, \dots, c_{2(M-1)}, c_{(2^{k-1}),0}, \dots, c_{(2^{k-1})(M-1)}\right],$$

$$\phi(x) = [\varphi_{10}(x), \dots, \varphi_{1(M-1)}(x), .., \varphi_{(2^{k-1})0}(x), \dots, \varphi_{(2^{k-1})(M-1)}(x)]^T,$$

$$\phi'(x) = [\varphi'_{10}(x), \dots, \varphi'_{1(M-1)}(x), .., \varphi'_{(2^{k-1})0}(x), \dots, \varphi'_{(2^{k-1})(M-1)}(x)]^T,$$

$$\phi''(x) = [\varphi''_{10}(x), \dots, \varphi''_{1(M-1)}(x), .., \varphi''_{(2^{k-1})0}(x), \dots, \varphi''_{(2^{k-1})(M-1)}(x)]^T,$$

Since there are $2^{k-1}M$ unknown coefficients, we need $2^{k-1}M$ algebraic equations. Depending on the type of the problem, we use the initial conditions

$$y(0) = D\phi(0) = k_1,\ y'(0) = D\phi'(0) = k_2.$$

To obtain two of the required equations. The other $2^{k-1}(M-2)$ equations are obtained by substituting the approximations in equation $y(x), y'(x)$ and $y''(x)$ in the given problem.

$$D\phi''(x) + \frac{a}{x}D\phi'(x) + f\big(x, D\phi(x)\big) = 0 \tag{15}$$

and then replacing x by the roots, x_i of the Taylor polynomials as collocation points

$$D\phi''(x_i) + \frac{a}{x}D\phi'(x_i) + f\big(x_i, D\phi(x_i)\big) = 0 \tag{16}$$

The system of equations together with the conditions can be solved by the Newton's iterative method and find the approximate solution of the given problem.

Consider the steady-state reaction-diffusion equation [28]

$$\frac{d^2c}{dx^2} - \frac{\phi^2 c}{1+c+\left(\frac{c^2}{\beta}\right)} = 0 \tag{17}$$

$$\frac{dc}{dx} = 0 \text{ at } x = 1 \text{ and } c = c_0 \text{ at } x=1 \tag{18}$$

$$c = 2a_0 + 8a_1x - 4a_1 + 32a_2x^2 - 32a_2x + 6a_2$$

Using the Taylor Wavelet Method (TSM) with $k = 1$ and $M = 3$ and using the collocation point $x = \frac{1}{2}$, we get $c = a_0 + \sqrt{3}a_1x + \sqrt{5}a_2x^2$ using given conditions; $a_0 = c_0 - \sqrt{5}a_2; a_1 = 0$.

5. Results and Discussion

We have successfully established the analytical expressions using the Chebyshev wavelet method (CWM) and Taylor wavelet method (TWM) for obtaining the analytical expressions with various values of the parameters. Our solutions have been validated with the results obtained by Chitra Devi et al. [28] using the numerical method (NM). The proposed results are also compared with those of the homotopy analysis perturbation method (HAPM) in Tables 5 and 7. For small parameter values of k and M, the results are very close to the results obtained by Chitra Devi et al. [28] results. For approximation results, we utilized the same values for the parameters as in [28]. The interval of Thiele modulus lies between 50–260, the interval of the ratio of substrate inhibition to Michaelis constant is 0.5–100, and the bulk concentration is in the range 0–1200.The proposed TWM solutions have been validated with the results obtained by Chitra Devi et al. [28]

The performance of the proposed analytical approach is evaluated by comparing the obtained results with those of the numerical method (NM) for both planar and cylindrical geometries under various parameter settings. Tables 1–4 present the variation of the dimensionless substrate concentration c for a planar particle under different combinations of bulk concentration c_0, Thiele modulus ϕ, and inhibition parameter β, while Tables 5–7 report the corresponding results for cylindrical particles. The comparison demonstrates that the proposed method exhibits excellent agreement with the numerical solutions across all tested parameter ranges. In particular, for both low and high values of β and ϕ, the deviation between the analytical and numerical results remains negligible, confirming the robustness and accuracy of the proposed technique in capturing the nonlinear behavior of substrate concentration profiles.

Table 1. Comparison of the proposed method and numerical method (NM) for dimensionless substrate concentration c of planar particle for c_0 = 1200, ϕ = 50 and various values of β = 0.1 and β = 20.

x	NM	TWM	%	CWM	%	TWM	%	*X*	NM	TWM	%	CWM	%	TWM	%
0.0	1199.90	1199.90	0.0	1199.90	0.0	1199.90	0.0	0.0	1179.20	1179.80	0.051	1179.16	0.0	1179.24	0.003
0.2	1199.90	1199.90	0.0	1199.90	0.0	1199.90	0.0	0.2	1180.03	1180.60	0.048	1179.99	0.0	1180.07	0.003
0.4	1199.92	1199.91	0.0	1199.91	0.0	1199.92	0.0	0.4	1182.53	1183.02	0.041	1182.49	0.0	1182.56	0.002
0.6	1199.94	1199.93	0.0	1199.93	0.0	1199.94	0.0	0.6	1186.70	1187.06	0.030	1186.66	0.0	1186.71	0.000
0.8	1199.97	1199.96	0.0	1199.96	0.0	1199.97	0.0	0.8	1192.52	1192.71	0.016	1192.50	0.0	1192.52	0.000
1.0	1200.00	1200.00	0.0	1200.00	0.0	1200.00	0.0	1.0	1199.99	1200.00	0.001	1200.00	0.0	1200.00	0.000

Table 2. Comparison of the proposed method and numerical method (NM) for dimensionless substrate concentration c of planar particle for c_0 = 1200, ϕ = 50 and various values of β = 40 and β = 70.

x	NM	TWM	%	CWM	%	TWM	%	*X*	NM	TWM	%	CWM	%	TWM	%
0.0	1158.50	1160.78	0.197	1158.31	0.0	1158.64	0.012	0.0	1127.70	1134.26	0.581	1127.00	0.0	1128.05	0.031
0.2	1160.17	1162.34	0.187	1159.97	0.0	1160.29	0.010	0.2	1130.62	1136.86	0.552	1129.92	0.0	1130.93	0.027
0.4	1165.17	1167.02	0.159	1164.98	0.0	1165.26	0.007	0.4	1139.37	1144.69	0.467	1138.68	0.0	1139.56	0.016
0.6	1173.49	1174.85	0.116	1173.32	0.0	1173.53	0.003	0.6	1153.91	1157.78	0.336	1153.28	0.0	1153.95	0.003
0.8	1185.10	1185.83	0.061	1184.99	0.0	1185.11	0.000	0.8	1174.16	1176.19	0.173	1173.72	0.0	1174.10	−0.005
1.0	1199.98	1200.00	0.002	1200.00	0.0	1200.00	0.000	1.0	1200.03	1200.00	0.003	1200.00	0.0	1200.00	0.000

Table 3. Comparison of Proposed method and numerical method (NM) for dimensionless substrate concentration c of planar particle for c_0 = 800, β = 0.5 and various values of ϕ =50 and ϕ = 140.

x	NM	TWM	%	CWM	%	TWM	%	X	NM	TWM	%	CWM	%	TWM	%
0.0	799.22	799.22	0.0	799.218	0.0	799.219	0.0	0.0	793.84	793.92	0.010	793.833	0.0	793.843	0.0
0.2	799.25	799.25	0.0	799.249	0.0	799.250	0.0	0.2	794.09	794.16	0.009	794.079	−0.001	794.089	0.0
0.4	799.35	799.35	0.0	799.343	0.0	799.344	0.0	0.4	794.83	794.89	0.008	794.819	−0.001	794.828	0.0
0.6	799.50	799.50	0.0	799.499	0.0	799.500	0.0	0.6	796.06	796.11	0.006	796.053	0.0	796.059	0.0
0.8	799.72	799.72	0.0	799.718	0.0	799.719	0.0	0.8	797.79	797.81	0.003	797.780	−0.001	797.783	0.0
1.0	800.00	800.00	0.0	799.999	0.0	800.000	0.0	1.0	800.00	800.00	0.000	800.000	0.0	800.000	0.0

Table 4. Comparison of Proposed method and numerical method (NM) for dimensionless substrate concentration c of planar particle for c_0 = 800, β = 0.5 and various values of ϕ = 190 and ϕ = 230.

x	NM	TWM	%	CWM	%	TWM	%	X	NM	TWM	%	Cheb	%	TWM	%
0.0	788.59	788.86	0.034	788.567	−0.002	788.604	0.001	0.0	783.18	783.76	0.074	783.131	−0.006	783.215	0.004
0.2	789.05	789.30	0.032	789.024	−0.003	789.060	0.001	0.2	783.86	784.41	0.070	783.806	−0.006	783.886	0.003
0.4	790.42	790.64	0.027	790.396	−0.003	790.427	0.000	0.4	785.88	786.35	0.060	785.830	−0.006	785.901	0.002
0.6	792.70	792.86	0.020	792.683	−0.002	792.707	0.000	0.6	789.25	789.59	0.044	789.203	−0.005	789.258	0.001
0.8	795.90	795.98	0.011	795.886	−0.001	795.897	0.000	0.8	793.96	794.14	0.023	793.927	−0.004	793.957	0.000
1.0	800.00	800.00	0.000	800.000	−0.000	800.000	0.000	1.0	800.00	800.00	0.000	800.000	0.00	800.000	0.000

Table 5. Comparison of the proposed method and numerical method (NM) for dimensionless substrate concentration c of cylindrical particle for c_0 = 1200, ϕ = 260 and various values of β =0.5.

x	NM	TWM	%	CWM	%	TWM	HAPM
0.0	1199.20	1198.31	−0.074	1199.16	−0.004	1198.31	1198.31
0.2	1199.23	1198.38	−0.071	1199.19	−0.004	1198.38	1198.38
0.4	1199.34	1198.58	−0.063	1199.29	−0.004	1198.58	1198.58
0.6	1199.50	1198.92	−0.049	1199.46	−0.004	1198.92	1198.92
0.8	1199.74	1199.39	−0.029	1199.70	−0.004	1199.39	1199.39
1.0	1200.04	1200.00	−0.004	1200.00	−0.004	1200.00	1200.00

Furthermore, the results indicate that variations in β and ϕ significantly influence the substrate concentration distribution, where higher Thiele modulus values lead to stronger diffusion–reaction limitations, resulting in a steeper decline in concentration. Similarly, changes in β affect the extent of substrate inhibition and consequently modify the concentration profiles within the particle. The consistency observed between planar and cylindrical geometries further validates the general applicability of the proposed method for different physical configurations. Overall, the close agreement between the analytical results and the numerical method confirms the reliability of the proposed approach for solving nonlinear reaction-diffusion problems.

Table 6. Comparison of proposed method and numerical method (NM) for substrate concentration c of cylindrical particle for $c_0 = 800$, $\phi = 90$ and various values of $\beta = 0.5$.

x	NM	TWM	%	CWM	%	TWM	%
0.0	778.40	779.34	0.121	778.309	−0.012	778.453	0.006
0.2	779.27	780.17	0.115	779.180	−0.012	779.315	0.005
0.4	781.87	782.64	0.098	781.785	−0.011	781.90	0.003
0.6	786.20	786.76	0.071	786.121	−0.011	786.21	0.000
0.8	792.25	792.54	0.037	792.192	−0.007	792.243	0.000
1.0	800.00	800.00	0.000	800.000	0.000	800.00	0.000

Table 7. Comparison of Proposed method and numerical method (NM) for substrate concentration c of cylindrical particle for $c_0 = 800$, $\beta = 5$ and various values of $\phi = 20$.

x	NM	HAPM	%	TWM	%	CWM	TWM
0.0	799.38	798.76	0.078	799.38	0.0	798.755	798.756
0.2	799.41	798.81	0.075	799.40	0.0	798.805	798.806
0.4	799.48	798.96	0.065	799.48	0.0	798.955	798.955
0.6	799.60	799.20	0.050	799.60	0.0	799.203	799.204
0.8	799.78	799.55	0.028	799.78	0.0	799.551	799.552
1.0	800.00	800.00	0.000	800.00	0.0	800.00	800.00

The graphical results presented in Figures 1–4 further support these findings. Figures 1 and 2 show the variation of the dimensionless substrate concentration c for planar particles under different values of β and ϕ, respectively, while Figures 3 and 4 present the corresponding comparisons for cylindrical particles under different combinations of c_0, β, and ϕ. In all cases, the proposed method shows excellent agreement with the numerical method, with nearly overlapping profiles throughout the domain. The plots also clearly indicate that increases in ϕ lead to sharper concentration gradients due to enhanced diffusion-reaction effects, while variations in β significantly alter the inhibition behavior and hence the concentration distribution. Overall, the strong agreement observed in both tables and figures confirms the accuracy, stability, and effectiveness of the proposed analytical method for nonlinear reaction-diffusion systems in both planar and cylindrical geometries.

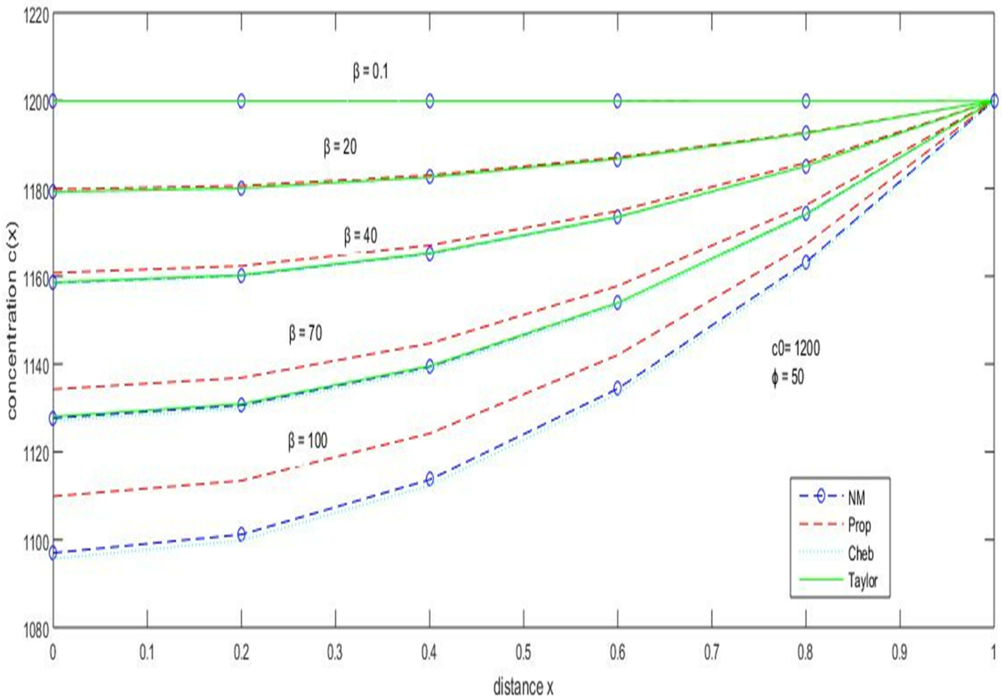

Figure 1. Comparison of the proposed method and numerical method (NM) for dimensionless substrate concentration c of planar particle for $c_0 = 1200$, $\phi = 50$ and various values of β.

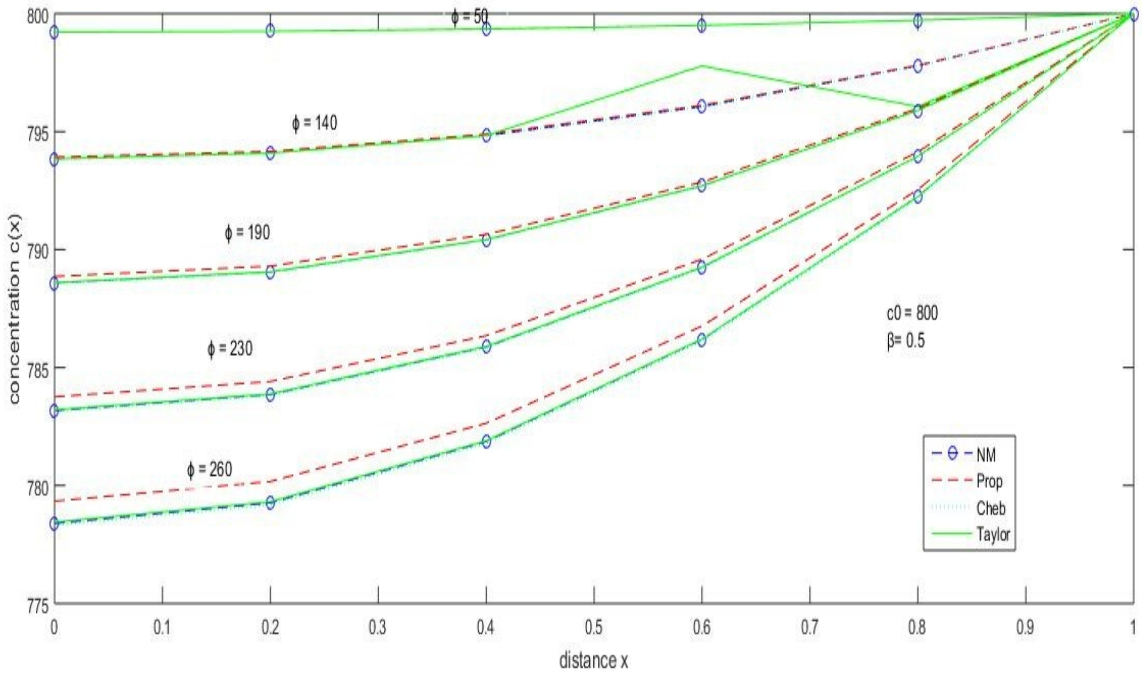

Figure 2. Comparison of proposed method and numerical method (NM) for dimensionless substrate concentration c of planar particle for c_0 = 800, β = 0.5 and various values of ϕ.

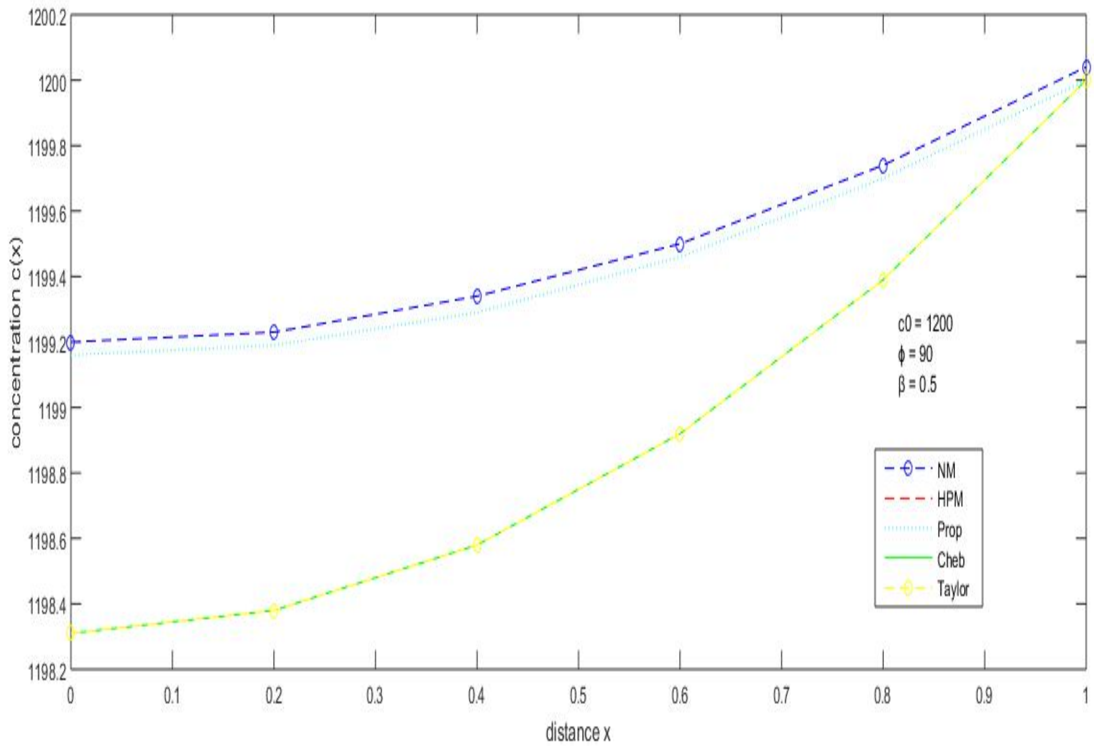

Figure 3. Comparison of proposed method and numerical method (NM) for substrate concentration c of cylindrical particle for c_0 = 1200, ϕ = 90 and various values of β.

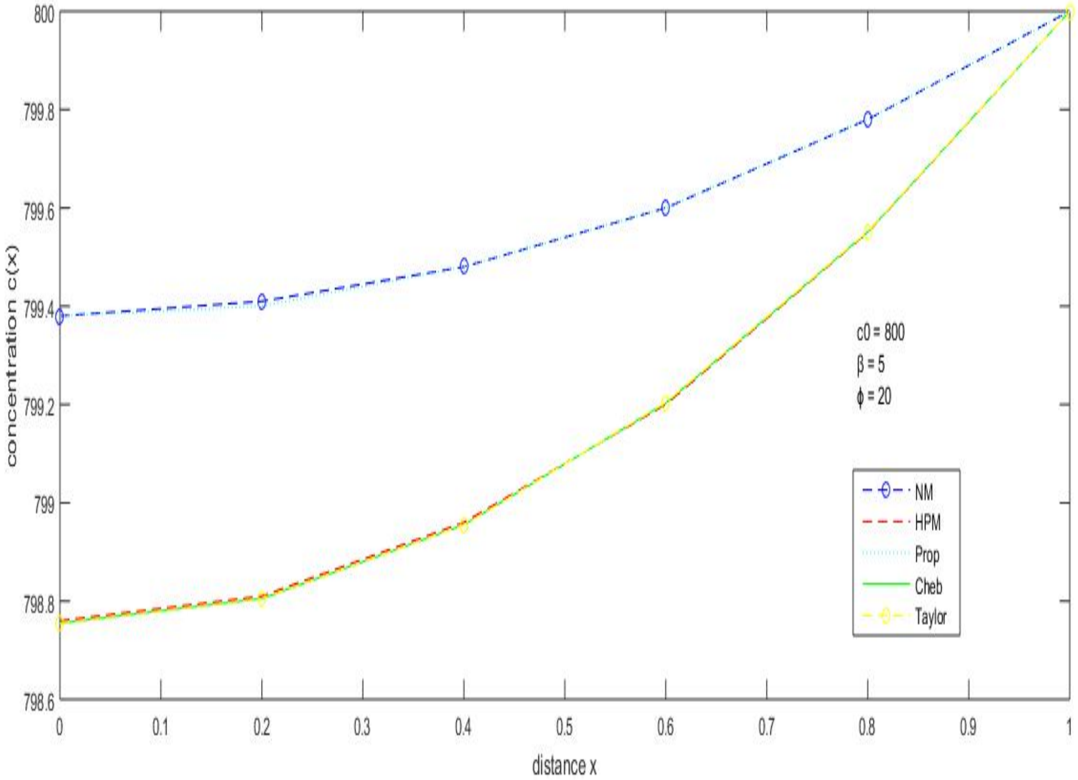

Figure 4. Comparison of Proposed method and numerical method (NM) for substrate concentration c of cylindrical particle for $c_0 = 800$, $\beta = 5$ and various values of ϕ.

6. Conclusions

In this research work, two reliable wavelet-based computational algorithms have been applied successfully to derive analytical expressions for the substrate concentration for all values of bulk concentration, Thiele modulus, and kinetic parameter, as well as for spherical, cylindrical, and planar particles. The proposed wavelet results have been validated against the numerical simulations obtained using the fourth-order Runge-Kutta (RK4) method and the Homotopy perturbation method (HPM). The results reveal that CWM and TWM are efficient and straightforward methods for investigating the numerical solutions of nonlinear reaction-diffusion models. These algorithms can be easily extended to solve other types of nonlinear steady and unsteady reaction-diffusion problems arising in bioprocess engineering. Another advantage of the proposed method is that it is simple and accessible to the wider research community, especially to those with less analytical background. An unsteady-state reaction-diffusion model for the prediction of surface coverage in biosensors is currently ongoing.

Author Contributions

K.H.: conceptualization, writing—original draft preparation, methodology; S.K.: Software, Visualization; R.S.: writing—reviewing and editing and G.H.: Supervision, Validation, Funding. All authors have read and agreed to the published version of the manuscript.

Funding

The authors are thankful to SASTRA Deemed University, Thanjavur for providing infrastructure support to carry out this research. We also acknowledge the DST-ANRF (CRG Grant) File Number: CRG/2023/002736, New Delhi for financial support.

Institutional Review Board Statement

Not applicable.

Informed Consent Statement

Not applicable.

Data Availability Statement

Data are contained within the article.

Conflicts of Interest

The authors declare no conflict of interest.

Use of AI and AI-Assisted Technologies

No AI tools were utilized for this paper.

References

1. Jesionowski, T.; Zdarta, J.; Krajewska, B. Enzyme immobilization by adsorption: A review. *Adsorption* **2014**, *20*, 801–821.
2. Oliveira, S.C. Evaluation of effectiveness factor of immobilized enzymes using Runge-Kutta-Gill method: How to solve mathematical undetermination at particle center point? *Bioprocess Eng.* **1999**, *20*, 185–187.
3. Fink, D.J.; Na, T.; Schultz, J.S. Effectiveness factor calculations for immobilized enzyme catalysts. *Biotechnol. Bioeng.* **1973**, *15*, 879–888.
4. Manjón, A.; Gómez, J.L.; Gómez, E.; et al. Evaluation of the effectiveness factor along immobilized enzyme fixed-bed reactors: Design of a reactor with naringinase covalently immobilized into the glycophase-coated porous glass. *Biotechnol. Bioeng.* **1987**, *30*, 491–497.
5. Vos, H.J.; Heederik, P.J.; Potters, J.; et al. Effectiveness factor for spherical biofilm catalysts. *Bioprocess Eng.* **1990**, *5*, 63–72.
6. Bódalo, A.; Gómez, J.; Gómez, E.; et al. Analysis of diffusion effects on immobilized enzymes on porous supports with reversible Michaelis-Menten kinetics. *Enzym. Microb. Technol.* **1986**, *8*, 433–438.
7. Gómez, J.L.; Bódalo, A.; Gómez, E.; et al. Two-parameter model for evaluating effectiveness factor for immobilized enzymes with reversible Michaelis–Menten kinetics. *Chem. Eng. Sci.* **2003**, *58*, 4287–4290.
8. Rani, J.; Sevukaperumal, S.; Rajendran, L. Analytical expression of effectiveness factor for immobilized enzymes system with reversible Michaelis-Menten kinetics. *Asian J. Sci. Appl. Technol.* **2015**, *4*, 10–16.
9. Avudainayagam, A.; Vani, C. Wavelet-Galerkin method for integro-differential equation. *Appl. Numer. Math.* **2000**, *32*, 247–254.
10. Goyal, K.; Mehra, M. An adaptive meshfree spectral graph wavelet method for partial differential equations. *Appl. Numer. Math.* **2017**, *113*, 168–185.
11. Guf, J.S.; Jiang, W.S. The Haar wavelets operational matrix of integration. *Int. J. Syst. Sci.* **1996**, *27*, 623–628.
12. Razzaghi, M.; Yousefi, S. Legendre wavelets operational matrix of integration. *Int. J. Syst. Sci.* **2001**, *32*, 495–502.
13. Keshavarz, E.; Ordokhani, Y. A fast numerical algorithm based on the Taylor wavelets for solving the fractional Integro-differential equations with weakly singular kernels. *Math. Methods Appl. Sci.* **2019**, *42*, 4427–4443.
14. Keshavarz, E.; Ordokhani, Y.; Razzaghi, M. The Taylor wavelets method for solving the initial and boundary value problems of Bratu-type equations. *Appl. Numer. Math.* **2018**, *128*, 205–216.
15. Toan, P.T.; Vo, T.N.; Razzaghi, M. Taylor wavelet method for fractional delay differential equations. *Eng. Comput.* **2021**, 37, 231–240.
16. Pirabaharan, P.; Chandrakumar, R.D.; Hariharan, G. An efficient wavelet based approximation method for estimating the concentration of species and effectiveness factor in porous catalysts. *MATCH Commun. Math. Comput. Chem.* 2015, *73*, 705–727.
17. Sivasankari, M.K.; Rajendran, L. Analytical expression of the concentration of species and effectiveness factors in porous catalysts using the Adomian decomposition method. *Kinet. Catal.* **2013**, *54*, 95–105.
18. Rajaraman, R.; Hariharan, G. An efficient wavelet based spectral method to singular boundary value problems. *J. Math. Chem.* **2015**, *53*, 2095–2113.
19. Hariharan, G.; Rajaraman, R. A new coupled wavelet based method applied to the nonlinear reactions diffusion equation arising in mathematical chemistry. *J. Math. Chem.* **2013**, *51*, 2386–2400.
20. Mahalakshmi, M.; Hariharan, G.; Kannan, K. The wavelet methods to linear and nonlinear reaction diffusion model arising in mathematical chemistry. *J. Math. Chem.* **2013**, *51*, 2361–2385.
21. Mahalakshmi, M.; Hariharan, G. An efficient Chebyshev wavelet based analytical algorithm to steady state reaction-diffusion models arising in mathematical chemistry. *J. Math. Chem.* **2016**, *54*, 269–285.
22. Mahalakshmi, M.; Hariharan, G. An efficient Wavelet Based Approximation Method onto steady state Reaction-Diffusion Model arising in Mathematical Chemistry. *J. Membr. Biol.* **2014**, *247*, 263–271.

23. Yousefi, S.A. Legendre wavelets methods for solving differential equations of Lane–Emden type. *Appl. Math. Comput.* **2006**, *181*, 1417–1442.
24. Yang, Y. Solving a nonlinear multi-order fractional differential equation using Legendre Pseudo-spectral methods. *Appl. Math.* **2013**, *4*, 113–118.
25. Mohammadi, F. An extended Legendre Wavelet method for solving differential equation with non-analytic solution. *J. Math. Ext.* **2014**, *8*, 55–74.
26. Hariharan, G.; Kannan, K. Review of wavelet methods for the solution of reaction–diffusion problems in science and engineering. *Appl. Math. Model.* **2014**, *38*, 799–813.
27. Hariharan, G.; Kannan, K.; Sharma, K.R. Haar wavelet in estimating the depth profile of soil temperature. *Appl. Math. Comput.* **2009**, *210*, 119–125.
28. Devi, M.C.; Pirabaharan, P.; Rajendran, L.; et al. An efficient method for finding analytical expressions of substrate concentrations for different particles in an Immobilized enzyme system. *React. Kinet. Mech. Catal.* **2020**, *130*, 35–53.